

PACS numbers: 42.25.Dd; 42.62.Be; 42.87.–d; 87.10.Rt; 87.64.Cc
DOI: 10.1070/QE2012v042n05ABEH014888

Blood group typing based on recording the elastic scattering of laser radiation using the method of digital imaging

A.A. Dolmashkin, V.A. Dubrovskii, I.V. Zabenkov

Abstract. **The possibility is demonstrated to determine the human blood group by recording the scattering of laser radiation with the help of the digital imaging method. It is experimentally shown that the action of a standing ultrasound wave leads to acceleration of the agglutination reaction of red blood cells, to formation of larger immune complexes of red blood cells, and, as a consequence, to acceleration of their sedimentation. In the absence of agglutination of red blood cells the ultrasound does not enhance the relevant processes. This difference in the results of ultrasound action on the mixture of blood and serum allows a method of blood typing to be offered. Theoretical modelling of the technique of the practical blood typing, carried out on the basis of the elastic light scattering theory, agrees well with the experimental results, which made it possible to plan further improvement of the proposed method. The studies of specific features of sedimentation of red blood cells and their immune complexes were aimed at the optimisation of the sample preparation, i.e., at the search for such experimental conditions that provide the maximal resolution of the method and the device for registering the reaction of red blood cells agglutination. The results of the study may be used in designing the instrumentation for blood group assessment in humans.**

Keywords: *blood typing, agglutination, light scattering, radiative transfer equation, Monte Carlo method.*

1. Introduction

Blood typing according to AB_0 or Rh (rhesus) system is one of the most often used tests of laboratory diagnostics. For example, annually in the USA blood transfusion centres from 150 to 200 million of such tests are performed [1]. In our country the annual number of blood typing tests may be estimated to approach 100 million. Naturally, such a rate of blood typing occurrence requires development of appropriate instrumentation, the blood-typing automatic machines (see, e.g., [2–10]).

Table 1 summarises the instrumentation for blood typing, known to the authors. Unfortunately, we have to state that, according to our data, no such blood-typing instruments are produced in our country. This fact makes the research in this direction to be an urgent problem.

A.A. Dolmashkin, V.A. Dubrovskii, I.V. Zabenkov V.I. Razumovsky Saratov State Medical University, Bol'shaya Kazach'ya 112, 410026 Saratov, Russia; e-mail: alal777@yandex.ru, doubrovski43@yandex.ru, zabenkoviv@gmail.com

Received 16 April 2012
Kvantovaya Elektronika **42** (5) 409–416 (2012)
Translated by V.L. Derbov

Table 1. Devices for instrumental human blood typing.

Device	Manufacturer	Country
Galileo Echo ™	ImmucorGamma	USA
PK7200® Automated Microplate System TANGO Benchtop Blood Bank Analyzer	Olympus Diagnostics	Japan
ORTHO AUTOVUE Innova/ Ultra System ORTHO ProVue™ Automated BloodBank Instrument	Ortho-Clinical Diagnostics Johnson & Johnson Company	USA
Automatic Analyzer WADiana Compact	Diagnostic Grifols S.A.	Spain
Auto Analyzer	Technicon Instrument Corporation	USA
Groupamatic	Centre National de Transfusion	France
Haemotyper	Tecan	Switzerland

The possibility to increase the resolution of optical instruments for blood typing by using the ultrasound (US) waves was considered in [11–15]. We recall that the resolving power may be understood as the ratio of the optical signal P_+, corresponding to the positive agglutination reaction (the serum is immunologically adequate to the group of the blood under study, agglutinates are produced) to the level of the optical signal P_-, corresponding to the negative agglutination reaction (the serum does not correspond to the given blood group, agglutinates are not produced). Obviously, the increase in the resolving power $K = P_+/P_-$ improves the reliability of blood group assessment. It is extremely important that the error in the blood sample group assessment must be completely ruled out. The only acceptable relaxation of these restrictions is that in some rare cases the device may be unable to assess the blood group of the analysed sample at all.

The physical principles of the instrumentation for blood typing may be different; however, as a rule, recording and mathematical processing of optical signals were implemented in the analogue regime. In our opinion, the method of digital imaging in application to blood typing is up-to-date and promising. This method allows appropriate digital mathematical processing of results, storage of the results in the computer memory, and presenting the results in the form of medical documents. The principal possibility of applying digital imaging to monitoring the processes of agglutination and sedimentation of agglutinates aimed at blood typing was considered in [16].

The goal of the present paper is to analyse the facilities offered by the combination of the US treatment of the blood–

serum reaction mixture, considered by the authors of the present paper earlier, with the digital recording and processing of the data, describing agglutination of red blood cells, as well as sedimentation of red blood cells and their agglutinates. Particular attention is paid to the modelling of the proposed method of blood typing and optimisation of sample preparation, aimed at improving the resolving power of human blood group assessment.

2. Object of study and experimental technique

The object of study was donor blood, mainly belonging to the second [A(II)] and the third [B(III)] groups, in combination with hemagglutinating serums, mainly of the types A_β(II) and B_α(III). It is necessary to note that in recent years the hemotransfusion stations often supply the clinics with so called concentrated red blood cells, i.e., blood with a certain amount of serum extracted by centrifuging, rather than with whole blood. The samples of concentrated red blood cells were studied in the present work. The concentration of red blood cells in these samples is nearly two times higher than in the whole blood. For brevity we shall refer them as blood samples. We recall that the blood of the group A(II) does not agglutinate with the serum A_β(II), i.e., the reaction is negative, but the blood A(II) + the serum B_α(III) produces agglutination of red blood cells, i.e., the reaction is positive. Similarly, B(III) + B_α(III) yields a negative reaction of red blood cells agglutination, but B(III) + A_β(II) yields a positive reaction. The adjustment of the experimental technique and the optimisation of sample preparation were carried out using these types of reactions. The agglutination reaction was implemented under different experimental conditions, namely, we varied the dilution rate of the studied blood samples and the blood-to-serum volume ratio, as well as the agglutination reaction type (positive or negative), etc. The total number of blood samples (donors) studied was 32, including 17 donors of A(II) group and 15 donors of B(III) group. With the multiple experimental conditions taken into account, the number of experiments with these blood samples approached a few hundred.

The serum was diluted with saline, into which the sample of the studied blood was introduced. In the experiments the volume ratio of whole blood to whole serum varied from 1:100 to 1:2, and the dilution rate of this mixture varied from 1:100 to 1:10. The obtained blood–serum solution was placed in a cuvette, mounted on a piezoelectric ceramic transducer, and exposed to ultrasound. The duration of US treatment in the present experiments varied from 15 to 240 s. To excite the piezoelectric ceramic transducer we used a GZ-112/1 generator with the amplifier, and its output voltage was controlled by means of a C1-79 oscilloscope. The generator was tuned in resonance with the frequency of the transducer (ν = 2.25 MHz), and its output voltage, applied to the piezoelectric ceramic, did not exceed 15 V, which provided the US effect on the red blood cells without their haemolysis.

In [11–15] it was shown that when the solution of the blood–serum mixture is exposed to the ultrasound, a standing US wave in the cuvette is produced, which causes concentration of red blood cells and their complexes in the vicinity of the wave nodes. As a result, the blood solution became periodically stratified, the spatial period being equal to half-wavelength ($\lambda/2$) of the US. The increase in the concentration of red blood cells yielded the enhanced probability of their interaction and, therefore, promoted the agglutination in the case if the reaction is positive. Both the rate of the agglutination reaction and the size of immune complexes of the red blood cell increased and, as a result, after switching the US generator off (i.e., after terminating the levitation of red blood cells and agglutinates) the rate of sedimentation of agglutinates became higher, and the studied medium became optically clearer.

If the agglutination reaction is negative, the red blood cells, concentrated in the node vicinities, form nonspecific aggregates that decay into individual red blood cells after switching the ultrasound off. Naturally, the sedimentation rate of free red blood cells is much higher than that of agglutinates, and the medium stays turbid during a long time. The difference in the value of the optical transmission coefficient of the studied samples in the cases of positive and negative reactions carries the information on whether the agglutination reaction has occurred or not, which is used for blood group assessment of the sample.

The optical scheme of the experimental setup is presented in Fig. 1. The radiation beam from the He–Ne laser (*1*) (LGN-207B) was widened with the telescopic system (*2*). The neutral light filters (*3*) attenuated the light to provide the appropriate regime of operation of the digital photographic camera (*7*). The light was passed through the vertically oriented optical slit (*4*) (width 2 mm, height 22 mm) and directed into the cuvette (*5*) with the studies liquid. After passing through the studied solution the beam arrived at the polychromatic CCD camera (*7*) (Logitec Quick Cam), connected with the personal computer (*8*). Note, that all settings of the CCD camera (mentioned below as a digital camera) were fixed and not changed during the experiments. On the cuvette the optical slit produced a light spot with the dimensions ~2×22 mm, while the dimensions of the inner cavity of the cuvette were 18×32×5 mm (volume ~2.8 mL).

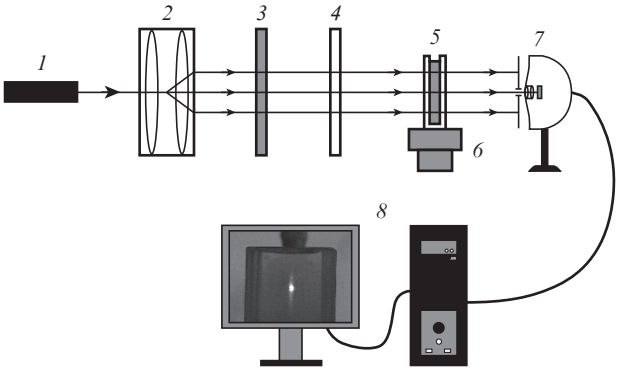

Figure 1. Optical scheme of the experimental setup:
(*1*) He–Ne laser; (*2*) telescopic system; (*3*) neutral light filters; (*4*) optical slit; (*5*) cuvette; (*6*) piezoelectric ceramic US transducer; (*7*) CCD camera; (*8*) computer.

The construction of the experimental setup (Fig. 1) allowed imaging and, therefore, quantitative determination of the radiation power distribution along the vertical direction at the output of the cuvette with the studied liquid (Fig. 2a), i.e., along the direction of sedimentation of red blood cells and their immune complexes. This, in turn, allowed determination of the optimal position of the probing beam in the y axis direction, for which the resolving power $K = P_+/P_-$ is maximal. Typical photographic images of the exit face of the cuvette, obtained by means of the digital camera (*7*) in the cases of positive and negative agglutination reaction, are presented in

Fig. 2. The stripes outlined by rectangles *D* are the areas of laser irradiation of the cuvette with the studied sample. Their shape and size are determined mainly by the geometry of the slit (*4*) (Fig. 1). The rectangles indicate the position and the size of the zone, selected for digital statistical processing of video images and used in the process of modelling.

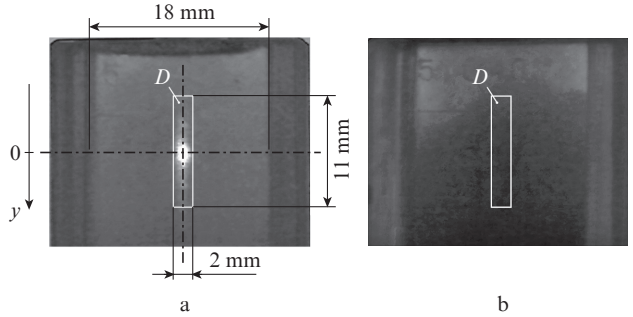

Figure 2. Typical photographs of the bright area of the cuvette with the studied solution for the case of positive (a) and negative (b) agglutination reaction of red blood cells. The rectangles select the zones of statistical processing of the experimental results and modelling of the experiment.

The procedure of mathematical processing of the photographs is based on pixel-by-pixel quantisation and presenting the result in the form of statistical samples [17]. For the 8-bit digital camera used in the present work, single-byte encoding of the state of each individual pixel allows recording of 256 colour hues, e.g., in the grey scale, from absolutely black ($B = 0$) to absolutely white ($B = 255$ units of brightness). The experiments with blood were preceded by testing the linearity of the colour characteristic of the digital camera, i.e., the dependence of the brightness B of the image, obtained using the digital camera, on the power P of the incident light flow (in milliwatts), measured with a calibrated Newport Power Meter 1815-c photodetector.

The obtained experimental results were approximated with cubic polynomials:

$$B(P) = 4\times10^{-6}P^3 - 4.2\times10^{-3}P^2 + 1.5P. \quad (1)$$

Using the personal computer, the measured function $B(P)$ was transformed into the inverse function $P(B)$, which was approximated by the polynomial, providing the best fit and having the form

$$P(B) = 5\times10^{-5}B^3 - 7.6\times10^{-3}B^2 + B. \quad (2)$$

The plot of the function (2) may be considered as a calibration curve of the digital camera. The results of further measurements were mathematically processed taking this dependence into account, which allows widening of the dynamical range of recorded light flows. Indeed, performing experiments with the entire light characteristic $B(P)$ leads to the distortion of results, and limiting the operation to the linear region only significantly reduces the dynamical range of the measurements. It seems worth noting, that in the experiments with biological objects, dynamically changing in time, when the optical transmission coefficient varies within wide limits, it is often impossible to ensure that after probing the biological object the light flow will fit the linear part of the light characteristic of the digital camera.

3. Results of experiments

The resolving power of the considered method of testing the agglutination reaction essentially depends on the choice of the region of the studied liquid to be probed with the laser beam. The experiments show that the optimal region lies within 9–13 mm (along the y axis) from the meniscus of the studied liquid. This position of the probing laser beam corresponds to the maximal value of the resolving power $K = P_+/P_-$. Figure 3 presents some of the experimental results in the form of dependences of the power of laser radiation, recorded by the digital camera, on the coordinate y in the case of positive (+) and negative (–) agglutination reactions. It is seen that the resolution K at the point $y = 0$ exceed 70 units. Thus is an evidence of the capability of the given device (Fig. 1) to provide reliable distinction between these two types of reaction.

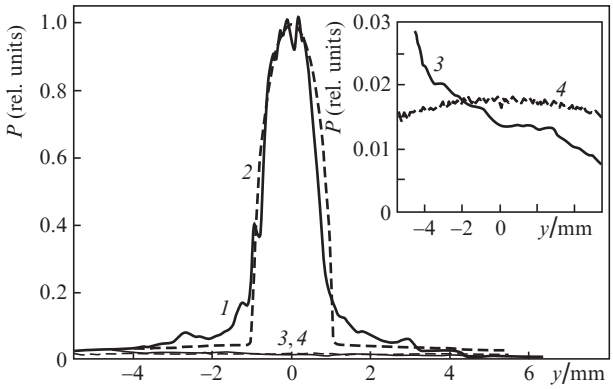

Figure 3. Experimental (*1*,*3*) and theoretical (*2*,*4*) dependences of the radiation power P, passed through the solution of the blood–serum mixture and incident on the photo camera, on the depth of the liquid layer y for the cases of positive (*1*,*2*) and negative (*3*,*4*) agglutination reactions. All data are normalised to the maximal power for the positive reaction of agglutination.

Samples of other blood groups were studied in a similar way. The typical results are summarised in Table 2 (the conditions of the experiments are discussed in Section 4).

In Table 2 (i) the experimental results obtained with the serum of the fourth blood group AB_0 are not presented, since it is known that this type of serum does not cause agglutination of red blood cells of any blood group (which is confirmed by our own experiments); (ii) in the calculation of K it was assumed that the negative reaction is the one, corresponding to the combination of the blood of the studied group and the serum of the fourth group, for which the agglutination reaction is always negative.

Table 2. Resolving power of the blood grouping device for different blood–serum combinations.

Blood group	Serum type		
	$0_{\alpha\beta}$(I)	A_β(II)	B_α(III)
0(I)	0.3	0.5	0.5
A(II)	**56**	3.5	**76**
B(III)	**82**	**67**	2.0
AB(IV)	**152**	**86**	**85**

Note: The K values given in boldface correspond to the blood–serum combinations, for which the agglutination of red blood cells must occur; the rest values correspond to principal absence of agglutination.

One can see from Table 2 that for the blood–serum combinations with possible agglutination the resolving power K is high enough; for different blood groups it varies from 56 to 152. In the case of the objective absence of agglutination the values of K are essentially lower, namely, from 0.3 to 3.5.

4. Modelling of blood typing method and experimental setup

The goal of the modelling was to reveal the causes of the difference in the recorded optical signals after passing of the laser beam through the cuvette with the studied samples in the cases of positive and negative reaction, to clarify the role of absorption and scattering of light by the samples, the competition of these phenomena, as well as to search for the ways of further improvement of the method of blood typing, proposed here.

A number of optical spectral measurements were performed before the modelling. These measurements were performed with the samples of the blood–serum solution [group B(III)] after ultrasonic treatment, incubation and relevanf measurements using the digital camera. Both for positive and negative agglutination reactions the samples were taken from the cuvette volume, corresponding to the middle of the area D (see Fig. 2). The initial blood–serum ratio in the mixture was 1:10, and then it was diluted with saline in the proportion 1:25. The choice of the proportions is justified in Section 5.

4.1. Optical spectral measurements

The spectra of overall reflection (R) and transmission (T) of the studied solutions were recorded by means of the two-beam PerkinElmer Lambda 950 spectrophotometer using the integrating sphere with correction of etalon reflection. To record the spectrum of the collimated transmission coefficient U we used four apertures, each having the diameter 1.5 mm, separated by the distances 5, 3, and 7 cm. The separation between the last aperture and the photomultiplier was 50 cm. The sample solutions were placed in the glass cuvette with the glass thickness 1 mm. The spectral characteristics found for the cases of positive and negative agglutination reaction are presented in Fig. 4.

To describe the transport of optical radiation and to determine the spectral dependences of the absorption and scattering indices of the studied samples we used the radiative transfer equation [18–20]:

$$\frac{\partial I(\boldsymbol{r},\boldsymbol{s})}{\partial \boldsymbol{s}} = -(\mu_a + \mu_s) I(\boldsymbol{r},\boldsymbol{s}) + \mu_s \int_{4\pi} \rho(\boldsymbol{s},\boldsymbol{s}')\, d\Omega'. \qquad (3)$$

Equation (3) describes the variation of the intensity $I(\boldsymbol{r},\boldsymbol{s})$ of light flow as a function of the position $\boldsymbol{r}$ and the direction $\boldsymbol{s}$, caused by to the energy decrease due to absorption and scattering, which are described by the indices of absorption μ_a and scattering μ_s, and by the energy increase due to the scattered light coming from all directions $\boldsymbol{s}'$. The function $\rho(\boldsymbol{s},\boldsymbol{s}')$ describes the indicatrix of single scattering.

To solve Eqn (3) and to find the spectral dependences of μ_a and μ_s, and the scattering anisotropy factor g, we used the adding-doubling method, implemented by the program iad [21]. The experimental spectra of R, T, and U (Fig. 4) were used as the input data of the program. The refractive index n of the cuvette walls was assumed to be 1.5. The spectral dependences

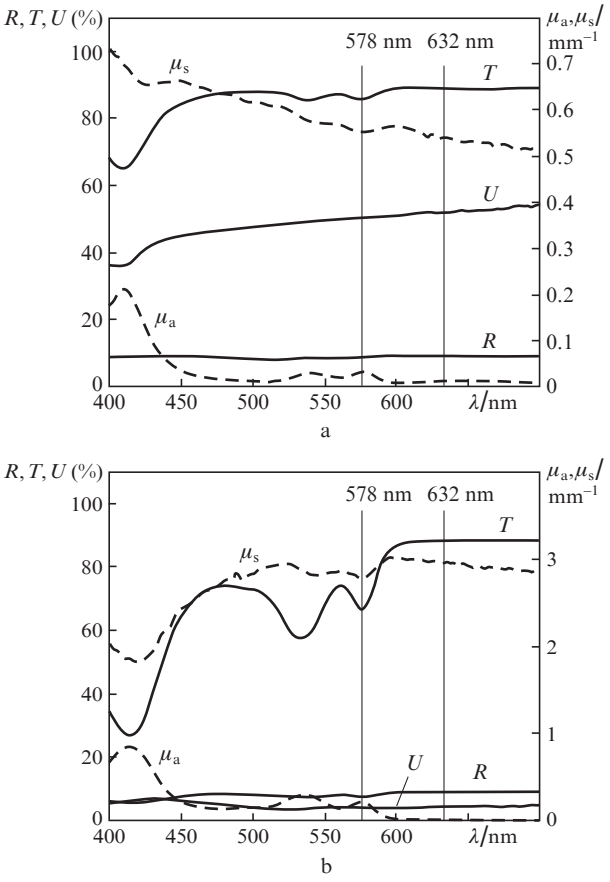

Figure 4. Spectra of measured overall reflection R, overall transmission T, and collimated transmission U coefficient of the studied solutions and the calculated absorption μ_a and scattering μ_s indices for positive (a) and negative (b) agglutination reactions. Vertical lines mark the wavelengths of He–Ne laser radiation (λ = 632 nm) and the maximum of haemoglobin absorption maximum in the green spectral region (λ = 578 nm).

of the absorption and scattering indices, calculated following this procedure, are also presented in Fig.4.

4.2. Modelling light transfer in the samples and its recording by the digital camera

Since the wavelength of the He–Ne laser used in the experiments belongs to the red spectral region, only the Red component of the RGB decomposition of the photographic images was analysed. To take the nonlinear sensitivity of the CCD matrix into account, the brightness of the pixels was converted from the units of brightness B into the units of power P in correspondence with the dependence (2) found above. The power of radiation at a certain fixed depth y in the cuvette was found by averaging the power along the corresponding line within the width of the rectangle D (see Fig. 2).

Under the conditions of our experiment on recording the agglutination reaction and using the solution of Eqn (3), we implemented the calculation of light transfer by means of the Monte Carlo method, which implies simulating the propagation of individual photons in a disperse medium. The light was presented by a set of N ballistic particles (photons), each having the statistical weight $1/N$ and being able to experience absorption or scattering in a certain direction (N was chosen to be 10^8). The events of scattering and absorption, as well as the choice of the propagation direction of photons, are drawn

Table 3. Optical characteristics of blood solutions, measured at the wavelengths $\lambda = 632$ and 578 nm for the cases of positive and negative agglutination reactions.

Wavelength/nm	Positive reaction			Negative reaction		
	μ_a/mm^{-1}	μ_s/mm^{-1}	g	μ_a/mm^{-1}	μ_s/mm^{-1}	g
632	0.0107	0.5417	0.9306	0.0135	2.9316	0.9839
578	0.0343	0.5500	0.9051	0.2238	2.7951	0.9629

using the random number generator. The number of scattering events for an individual photon increases with the growth of μ_s in comparison with μ_a, and with increasing medium thickness. The integral spectral characteristics of the sample are obtained by statistical averaging over a large number of photons. To take the multilayer structure of the sample into account, i.e., the cuvette walls and the solution itself, we used the modification of the Monte Carlo method, described in [22]. In the calculations the thickness of each wall of the cuvette was set to be 1 mm, and its inner cavity thickness was taken to be 5 mm. The refractive index of the glass, of which the cuvette was made, was assumed to be $n = 1.5$, and the refractive index of the solution was taken to be $n_{sol} = 1.34$. The indices of absorption μ_a and scattering μ_s at the wavelength $\lambda = 632$ nm of the radiation from the He–Ne laser, as well as the scattering anisotropy factor g of the solution samples, used in the calculations, in the cases of positive and negative agglutination reaction are presented in Table 3. In this Table the optical characteristics of the same samples are also presented in the case of $\lambda = 578$ nm, corresponding to the maximum of absorption of light by haemoglobin in the green spectral region, for which similar modelling was carried out. The reasons for choosing this wavelength consist in the following.

In the experiment with the samples, exposed to He–Ne laser radiation, the photographs are strongly different in the cases of positive and negative reaction (see Fig. 2). As seen from Fig. 4, at the wavelength 632 nm (red light) μ_s exceeds μ_a by more than 200 times (negative reaction) and by more than 50 times (positive reaction), i.e., the attenuation of the light flow in the samples is mainly due to the light scattering. At the wavelength 578 nm (green light) the absorption index is essentially higher than in the red spectral region, so that for negative reaction μ_s exceeds μ_a only by nearly 10 times for both samples, the magnitude of scattering being nearly the same as in the red spectral region. Therefore, with the multiple scattering taken into account, at the absorption maximum wavelength the light absorption is expected to provide an essential contribution to the additional attenuation of light by the sample. This means that at the wavelength $\lambda = 578$ nm it is natural to expect a higher resolution $K = P_+/P_-$ than at $\lambda = 632$ nm.

To obtain the distribution of the radiation power, received by the photodetector, over the cuvette depth y, the geometrical parameters were taken into account in the modelling, namely, the separation between the cuvette and the photodetector (70 mm) and the aperture of the latter (2 mm). The presence of the optical slit having the dimensions 2×22 mm that spatially filters the radiation, incident on the cuvette in the optical scheme, required introducing a light source function into the model. Since the form of the spatial dependence of light intensity in the beam is unknown, in the calculations the assumption was used that the area of the sample with the dimensions 2×22 mm was illuminated uniformly. The results of the calculations ($D = 11$ mm) are presented in Fig. 3 together with the experimental data. It is seen that the results of calculations agree quite well with the experimental results. For positive reaction a distinct peak is seen having the width ~2 mm, which coincides with the size of the digital camera aperture. This is a manifestation of the fact that the peak is produced by photons that pass through the sample without scattering and absorption. The scattered photons are responsible for the presence of small lobes at the wings of the peak.

As shown by the calculations, for negative reaction (Fig. 3) practically all the light is scattered and produces uniform illumination of the photographic camera objective by the light coming from all regions of the zone D. Slight difference between the experimental and calculated curves is due to the fact that in the experiment, after a certain period of incubation, some part of red blood cells experienced sedimentation, thus making the transmission in the top part of the cuvette with the solution greater than in the bottom part. In our model the effect of sedimentation of red blood cells was not taken into account. Nevertheless, the fact that for negative reaction theoretical and experimental curves are at the same level is also a manifestation of good quantitative agreement between the results of modelling and experiment.

Similar to Section 2, in the process of modelling the method and the experimental setup for blood typing, the differentiation between the positive agglutination reaction and the negative one was made on the base of evaluating the coefficient $K = P_+/P_-$ (resolution), where P_+ is the power in the maximum of the curve for positive reaction and P_- is the power in the middle of the studied area D (see Fig. 3), so that K was the diagnoctic parameter. The values of K, calculated for $\lambda = 632$ and 578 nm, amount to 56.5 and 604, respectively, while the experimental value of K for $\lambda = 632$ nm is 73.5. The satisfactory agreement between the theoretical and experimental values of K at $\lambda = 632$ nm is worth attention. Moreover, as the theory shows, there are good perspectives to increase the resolving power by using probing light beams with the wavelength in the green part of the spectrum ($\lambda = 578$ nm).

5. Optimisation of preparation of blood–serum samples

Aimed at optimising the experimental technique and increasing the resolving power $K = P_+/P_-$ a special attention was paid to the questions of sample preparation. It is well known that in the 'hand-operated' blood typing the blood-to-serum ratio generally accepted in medical practice is 1:10. However, for instrumental blood typing this ratio may appear not optimal and requires testing. To this end, we obtained the dependence of the resolving power K on the blood-to-serum ratio with the rate of the mixture dilution 1:50, the duration of ultrasonic treatment being 60 s. In this case the incubation time t_{inc} was varied as a parameter and took the values 0, 30, 90, or 120 s. (The incubation time is the time passed from the moment of ultrasound shutoff [beginning of sedimentation of red blood cells and complexes] till the moment of the object photographing.)

One can see from Fig. 5 that the optimal blood-to-serum ratio lies in the interval from 1:5 to 1:10. The choice of such ratio provides substantial gain in the value of resolving power, when recording the agglutination reaction. In further experiments the blood-to-serum ratio was kept to be 1:10. Note, that the curves in Fig. 5 possess the shape analogous to that of precipitation curves, known in immunology. This fact allows an assumption that the range of blood-to-serum ratios from 0.1 to 0.2 corresponds to the zone of equivalence [23, 24].

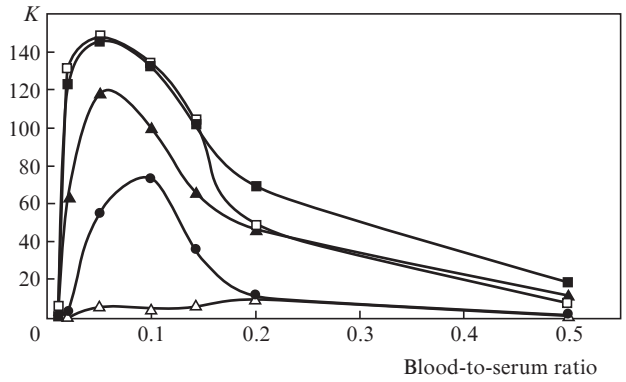

Figure 5. Dependence of resolution K on the blood-to-serum ratio for t_{inc} equal to 0 (△), 30 (●), 60 (▲), 90 (□) and 120 s (■).

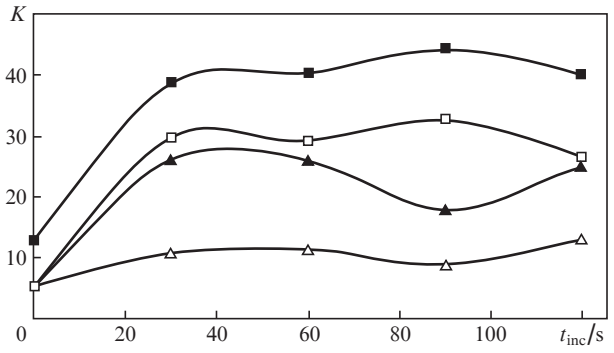

Figure 7. Dependences of the resolution K on the incubation time t_{inc} of the blood–serum mixture solution for the rates of dilution with saline 0.01 (△), 0.02 (▲), 0.04 (■) and 0.08 (□).

It is interesting to analyse the dependence of the resolution K on the duration of ultrasonic treatment t_{us} on the blood-serum mixture. The results are presented in Fig. 6. It is seen that the optimal duration of the ultrasonic treatment is 60 s. Further increase in t_{us} makes the resolution K lower. This is because for negative reaction longer ultrasonic treatment of the solution promotes the formation of larger 'non-specific' aggregates of red blood cells and, therefore, the increase in the sedimentation rate. Finally, this leads to the liquid clearing (increase in the power P_-) and the reduction of K.

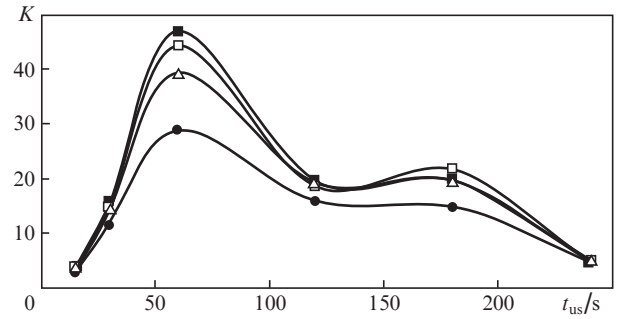

Figure 6. Dependences of the resolution K on the time of ultrasound action on the solution of blood–serum mixture at t_{inc} equal to 0 (△), 30 (●), 60 (▲), 90 (□) and 120 s (■).

Figure 7 illustrates the dependences of the resolution K on the time of incubation t_{inc} of the blood–serum solution under varying the rate of dilution with saline from 1:100 to 8:100. The limits of the dilution rate and the incubation time variation are dictated by the results of earlier papers [11–14]. One can see from Fig. 7 that the resolving power is growing till t_{inc} = 40–60 s, and then depends on the incubation time very weakly.

Such a behaviour of the dependences is explained by the fact that the increase in the incubation time for positive reaction leads to greater clearing of the mixture solution, i.e., an increase in P_+, while P_- is practically not changing, since the sedimentation of 'free' red blood cells is slow. As a result, the value of K increases. However, to the 60th second of incubation the sedimentation of large immune complexes of red blood cells is mainly finished, so that the value of P_+ becomes stabilised and the resolution K stops changing.

The dependences in Fig. 8, based on the results of Fig. 7, demonstrate the optimal values of the blood–serum mixture dilution rate for different incubation times. It is seen that the value of K is essentially dependent on the specific features of sample preparation: under the present experimental conditions 1:25 appeared to be the optimal dilution rate, which is close to the results of [11–14], obtained using analogue recording rather than digital one.

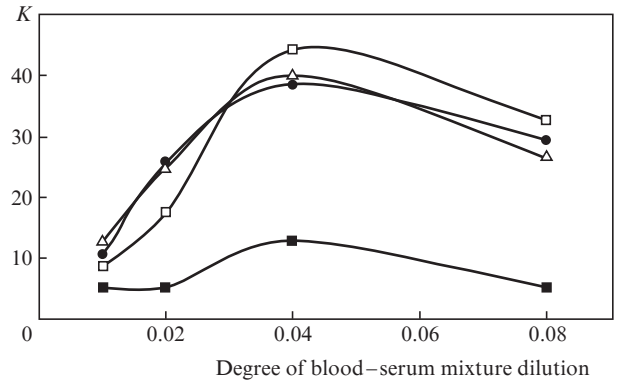

Figure 8. Dependences of the resolution K on the degree of dilution of the blood–serum mixture with saline for t_{inc} equal to 0 (■), 30 (●), 90 (□) and 120 s (△).

The performed experimental studies (see Figs 5–8) yield the choice of optimal conditions (Table 4), under which the resolving power of blood typing by means of the considered 'acoustooptical' method in its present implementation is maximal. Note, that the experimental results, presented in Fig. 3, were obtained under the experimental conditions, summarised in Table 4.

Table 4. Recommended values of parameters, providing the maximal resolving power of blood group assessment using the considered 'acousto-optical' method in its present implementation.

Experimental condition for the blood–serum mixture	Recommended value
The ratio of components	1:5–1:10
Time of exposure of the mixture solution to US	60 s
Dilution rate of the mixture	1:25
Incubation time of the irradiated mixture	90 s

6. Discussion

First, it is useful to discuss the questions of accuracy of measurements and reliability of blood group assessment. These questions are mutually connected; however, one should not put the sign of equality between them. Since, as a rule, in the experiments with biological objects there are no etalons, the accuracy of measurements in biomedicine is often associated with the reproducibility of the results of multiply repeated measurements for the same object and under the same experimental conditions. Exactly in this way the authors of [25] performed testing and comparison of blood typing results using the PK-7200 Olymp Group and Olymp Group II instruments. Similarly, in the present paper, in order to determine the reproducibility of results, we carried out five experiments for each of the reactions: the positive reaction A(II) + B_α(III) and the negative one A(II) + A_β(III) with determination of the resolving power K. The root mean square deviation $\sigma(K)$ from the mean value $K_{av} = 50$ was ± 7, which seems quite satisfactory for the work with biological objects.

The question of reliability of blood typing is more difficult because of extremely wide specificity of blood samples taken from different donors, even when these samples belong to the same group. Naturally, the reliability of blood group assessment increases with the growth of the resolving power K of the method. However, the value of K depends on a variety of factors, e.g., agglutination activity of red blood cells, concentration of red blood cells in the sample, haemoglobin content, viscosity of the studied blood, titer of the hemagglutinating serum, etc. Therefore, certain deviations of the resolution K from the mean value K_{av} appear in the course of experiments on optimising the blood typing technique (Figs 5–8). Note that the experimental points presented in these Figures are mean values, each obtained by averaging the individual results of K measurement in 14–18 blood samples from different donors (Section 2). The analysis has shown that under the optimal conditions, summarised in Table 4, the relative deviation of the resolution K from its average value over the donor group amounts to $\Delta K/K_{av} \approx 20\%$. However, in rare cases one can meet blood samples, for which the value of K appears to be significantly lower than presented in Table 2. As a rule, this may be due to weak agglutination activity of the red blood cells of the particular sample, as well as to other causes. That is why practically, as a result of thorough technical and medico-biological testing, the designers of blood typing instrumentation not only try to provide the maximal possible value of the resolution K, but also establish definite threshold values of K. In our paper these values are K_{th}^{max} and K_{th}^{min}, in other papers, e.g., in [6, 7], the authors make use of different threshold values. If for the blood sample under study $K > K_{th}^{max}$, then the agglutination reaction is assessed positive, if $K < K_{th}^{min}$, the reaction is negative. The group of the studied blood sample is assessed on the base of a sequence of such experiments with the same blood sample but different serums. If the measured value of the resolution K in an experiment with at least one of four serums appears in the zone of 'uncertainty' $K_{th}^{min} \leqslant K \leqslant K_{th}^{max}$, then it is impossible to draw a conclusion about the agglutination reaction. In this case the blood group is not assessed, and the issue of primary importance is that the instrument must definitely reply 'the blood group is unknown'. Such approach is generally accepted, since an error in blood typing during transfusion may cause a lethal outcome.

Consider some examples of this approach. The results of testing of the instrument, developed by the authors of [26] for blood group assessment using the systems AB_0 and Rh, were compared with those of parallel blood typing by means of the Technicon AutoAnalyzer instrument, and also, for control in some cases, using a 'hand-operated' (non-instrumental) method. The comparison has shown that in 97.3% of cases both instruments unambiguously assessed the blood group of 10042 samples, and only in 266 cases the answer of the instruments was 'blood group not assessed'. In these cases the blood group was verified by hand using the method of inverse testing.

In [27] the testing similar to [26] was performed with the instrument Inverness Blood Grouping System (IBG System). The results of measurements obtained using this instrument were compared with those obtained 'by hand'. Only in three cases of 2051 the result of blood typing returned by the IBG System was different from that obtained by hand-operated blood typing. In 86.1% of cases the results of IBG System were obtained without any additional technological interference [27].

Naturally, the increase in the resolving power of the blood typing instrument increases the deviation of the result of K measurement from the chosen interval $K_{th}^{min} - K_{th}^{max}$. Therefore, the reliability of the blood typing is increased, and the number of blood samples with unascertained group is reduced.

From the presented examples [26, 27] it is seen that establishing the interval $K_{th}^{min} - K_{th}^{max}$ and performing corresponding tests requires performing thousands, and sometimes even tens of thousands of experiments, which, naturally was not the goal of this work. At the same time we would like to note, that our goal is achieved. Indeed, we have shown that the combination of ultrasound action on the blood–serum mixture, considered by the authors of this paper earlier [11–15], with digital recording of the processes of agglutination of red blood cells, sedimentation of red blood cells and their agglutinates, followed by digital processing of the results, offers promising values of the resolving power of the 'acoustooptical' method and device. Besides that, from the performed studies we draw the optimal experimental conditions, under which the resolving power of the device in its present implementation is maximal. The modelling carried out outlines the way to future essential increase of the resolving power of the device.

7. Conclusions

The combination of ultrasonic treatment of the blood–serum reaction mixture with digital recording of sedimentation of red blood cells and their agglutinates allows attaining high values of resolving power when recording the reaction of agglutination of red blood cells. The optimal conditions of blood typing by means of the proposed 'acoustooptical' method are determined. The modelling of the experimental technique on the base of light scattering analysis allowed quantitative determination of the prospects of developing the method towards further increase of the resolving power and, therefore, improving the reliability of blood group assessment. The results of the study may be used in manufacturing devices for instrumental human blood typing.

Acknowledgements. The authors express their gratitude to V.I. Kochubey for affording an opportunity to work with spectral instrumentation and for valuable advice.

References

1. Vyas G.N. et al. United States Patent 5,776,711, July 7, 1998.
2. Sturgeon P. *Immunohematology*, **17**, 4 (2001).
3. Kline T.R., Runyon M.K., Pothiawala M., Ismagilov R.F. *Anal. Chem.*, **80** (16), 6190 (2008).
4. Muranyi I. et al. United States Patent 4,533,638, August 6, 1985.
5. Dubrovskii V.A., Dvoretskii K.N., Scherbakova I.V., Balayev A.E. *Prib. Tekh. Eksp.*, **42** (2), 111 (1999).
6. Steven R.A. *A Simplified Visible/Near-Infrared Spectrophotometric Approach to Blood Typing for Automated Transfusion Safety*. Thesis presented to North Carolina State University (Raleigh, North Carolina, USA, 2005).
7. Lambert J.B. *Miniaturized Device for Blood Typing Using a Simplified Spectrophotometric Approach*. Thesis submitted to North Carolina State University (Raleigh, North Carolina, USA, 2006).
8. Moncharmont P., Plantier A., Chirat V., Rigal D. *Immunohematology*, **19** (2), 54 (2003).
9. Goldfinger D. et al. United States Patent 4,650,662, March 17, 1987.
10. Battrell C.F. et al. United States Patent 20100112723. Publication date: 05/06/2010.
11. Alipov A.N., Vaninskii V.Z., Denisov L.B., Donskov S.I., Dubrovskii V.A., Zavyalo E.N., Knyaz'kov N.N. Inventors' Certificate No. 1683760 with priority of 04.06.1987.
12. Doubrovski V.A., Kirichouk V.F., Scherbakova I.V. *Abstr. Intern. Conf. Biomed. Opt. Europ. 94* (Lille, France, 1994) p. 60.
13. Dubrovskii V.A., Dvoretskii K.N. *Opt. Spektrosk.*, **89** (1), 109 (2000).
14. Doubrovski V.A., Dvoretski K.N. *Ultrasound in Medicine & Biology*, **26** (4), 655 (2000).
15. Dubrovskii V.A., Dvoretskii K.N., Balayev A.E. *Akustoopt. Zh.*, **50** (2), 184 (2004).
16. Gonzalez R.C., Woods R.E. *Digital Image Processing* (Upper Saddle River, NJ: Prentice Hall, 2008).
17. Dubrovskii V.A., Dolmashkin A.A. *Opt. Spektrosk.*, **109** (2), 1346 (2010).
18. Chandrasekhar S. *Radiative Transfer* (New York: Dover, 1950).
19. Ishimaru A. *Wave Propagation and Scattering in Random Media* (New York: Wiley-IEEE Press, 1999).
20. Tuchin V.V. (Ed.) *Handbook of Optical Biomedical Diagnostics* (Bellingham: SPIE Press, 2002).
21. Prahl S.A., van Gemet M.J.C., Welch A.J. *Appl. Opt.*, **32** (4), 559 (1993).
22. Wang L., Jacques S.L., Zheng L. *Comp. Meth. Progr. Biol.*, **47**, 131 (1995).
23. Boyd W.C. *Fundamentals of Immunology* (New York: Interscience Publishers, Inc., 1943).
24. Roitt I.M. *Essential Immunology* (London: ELBS/Blackwell Scientific Pub., 1988).
25. Moncharmont P., Plantier A., Chirat V., Rigal D. *Immunohematology*, **19** (2), 54 (2003).
26. Chung A., Birch P., Ilagan K. *Transfusion*, **34** (1), 88 (1994).
27. Mintz P.D., Anderson G., Barasso C., Sorenson E. *Immunohematology*, **10** (2), 60 (1994).